

# EXPERIMENTAL ANALYSIS OF A SCREW-GLUED SHEAR CONNECTION FOR USE IN MASS TIMBER COMPOSITE PANELS

Tyler Hull<sup>1</sup>, Daniel Lacroix<sup>2</sup>

**ABSTRACT:** Ribbed or box section mass timber composite (MTC) panels offer a potential solution to the floor span limitations of conventional mass timber panels due to vibration. Glued connections have shown to be a viable shear connection in MTCs due to their high strength and stiffness. Investigated herein is the behaviour of a screw-glued connection of commercially available construction adhesive and self-tapping screws, to assess its viability to adequately transfer forces between the flanges and webs of MTCs. Shear tests on four 400mm long dimensional lumber T-sections yielded an average slip modulus of 17.63N/mm per mm<sup>2</sup> of glue, with an average yield stress of 4.59MPa and 3.47MPa from two bilinear data fit models. The connection was used to fabricate six 1.8m long dimensional lumber T-beams which were tested in flexure and used to validate a numerical model capable of capturing the behaviour. The results agreed well, with the average experimental midspan deflection being 0.98 of the average numerical midspan deflection. Overall, when used on a 10m HMT panel, analytical results using the  $\gamma$ -method indicated a nearly fully composite shear connection was achieved, and a vibration-controlled span of 10.4m was possible for the 455mm deep section.

**KEYWORDS:** Mass timber composite, screw-glued, shear connection, shear testing, experimental analysis

## 1 INTRODUCTION

### 1.1 BACKGROUND

Conventional mass timber flat slab floor systems, such as cross-laminated timber (CLT) panels on glulam beams, have difficulty rivalling the column spacing standard achieved by other commercially available floor systems due to the mass timber slab spans being limited by vibration and human comfort [1,2]. To achieve long floor spans using an all-wood system in structures where larger and open floor plans are needed (e.g., office, institutional, and high-end residential), designers have employed mass timber composite (MTC) ribbed (i.e., T-beams) and box (i.e., I-beams/hollowcore) panel floor systems (e.g., Catalyst, Spokane, WA, USA [3]; WoodIn, Waterloo, ON, Canada [4]). Figure 1 shows an example of a MTC ribbed panel consisting of a CLT panel for the flange that is connected to glulam webs through shear connections.

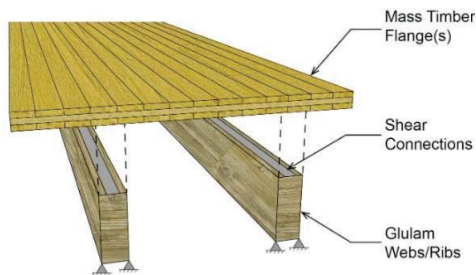


*Figure 1: Mass Timber Composite Ribbed Panel*

MTCs have shown the viability to overcome the current vibration and serviceability limitations of conventional mass timber flat slab floor systems (i.e., exceeding 7-8m), and be a viable all-wood long span floor system solution [5]. However, the shear connection (e.g., glue, self-tapping screws (STS)) has a crucial role in the transfer of forces between the flange(s) and the web. Due to vibration concerns at serviceability limit states often being the governing criteria in the design of MTCs, the shear connection's stiffness is critical to the overall element performance. Research has shown that glued connections [6] exhibit the highest shear connection stiffness; however, little research has been done on the types of glue to use, clamping procedures, and stiffnesses achieved in order to produce commercially viable bonds.

Montgomery [6] conducted a wide-ranging experimental study investigating the performance of 24 different shear connection options for hollowcore mass timber (HMT) panels through uniaxial tests on small-scale components and used the connection stiffness to numerically investigate their effects on, the behaviour of a 12.2 long HMT panel. It was observed that stiffer shear connections were necessary to achieve near fully composite action between the elements, thereby maximizing the efficient use of materials in the HMT panel, in addition to meeting the requirements for a 12.2m span. The identified connections were comprised of STS driven at an angle (30-45°), glue pressed, screw-glued, and perforated metal

<sup>1</sup> Tyler Hull, PhD Candidate, University of Waterloo, Waterloo, Canada, tyler.hull@uwaterloo.ca

<sup>2</sup> Daniel Lacroix, Assistant Professor, University of Waterloo, Waterloo, Canada, daniel.lacroix@uwaterloo.ca

plates with adhesive. Connections such as STS driven vertically (90°) were reported to not produce the needed stiffness to efficiently achieve adequate vibration performance at long spans [6]. Chen and Lam [7] investigated the performance of STS at 90° through numerical modelling and experimental testing on box panels comprised of CLT as top and bottom flanges, and dimensional lumber for the webs. As a result of the connection stiffness, the overall section exhibited minimal composite behaviour resulting in a highly non-linear stress distribution over the depth of the section, and tensile failure in the webs occurring rather than in the bottom flange [7]. While this connection proved to not be optimal for achieving the composite action needed for long span MTCs, good agreement was demonstrated between the numerical model and experimental results, thereby indicating the viability of numerical methods for predicting the behaviour of MTCs [7].

Jacquier and Girhammar [8] investigated CLT-glulam T-beams in bending for the purpose of developing a cassette (i.e., box) composite floor slab for use in multi-storey CLT buildings. In their study, STS driven at 45°, doubled-sided punched metal plates (DSNP), screw-glued, and a combination of STS and DSNP were utilized for the shear connection between the flange and web. The results between the experimental and predicted bending stiffness determined using the gamma ( $\gamma$ )-method, which is introduced in Annex B of Eurocode 5 [9], agreed reasonably well with the experimental results [10], thereby indicating that analytical methods such  $\gamma$ -method can be used to predict the stiffness of MTCs in design. This observation was also confirmed by Hull and Lacroix [11] who compared the results of the  $\gamma$ -method to finite element modelling results. The  $\gamma$ -method was able to reasonably accurately predict the bending stiffness of the MTC panel, with the main difference between the finite element model and  $\gamma$ -method being attributed to shear lag effects observed in the flanges [11].

Despite the fact that initial studies have showcased the potential of MTCs to be designed to meet long floor spans in a laboratory and numerical setting, adoption of mass timber long span floor systems by the industry has been hindered in large part due to the complications associated with implementing viable shear connections in manufacturing processes, particularly glued connections. This is primarily due to the fact that the glue bond can vary greatly depending on the type of glue used, the contact pressure, the glue line thickness, and environmental conditions during the assembly. Screw-gluing was shown to be a viable option for utilizing the high shear stiffness of glued connections without the need for large hydraulic presses [6,12]. However, the practical application of screwed gluing in manufacturing applications has been limited by the lack of knowledge on possible adhesive and screw configurations.

## 1.2 OBJECTIVES

The overarching aim of the larger research program is to develop fundamental knowledge of mass timber composites (MTCs) and the effects of connection

detailing on their behaviour in order to develop design guidelines and aid in their adoption by industry. The research specific objectives of this study are to: 1. investigate the shear behaviour of a screw-glued connection made with a commercially available construction adhesive, 2. establish the flexural behaviour of dimensional lumber T-beams using the screw-glued connection, 3. validate a finite element model capable of capturing the connection behaviour and predict the flexural response of the T-beams, and 4. investigate the potential span capabilities of MTC panels using the screw-glued connection analytically. Due to the limited information on the behaviour of connections and the effects of stiffness on the degree of composite action, as well with relatively higher associated costs with mass timber products, dimensional lumber was chosen to first investigate the behaviour and feasibility of the screw-glued connection in MTC panels.

## 2 SHEAR PERFORMANCE OF SCREW-GLUED CONNECTION USING DIMENSIONAL LUMBER

### 2.1 METHODOLOGY

The potential of using screw-glued connections in MTCs is first evaluated on a total of four specimens consisting of dimensional lumber. The shear connection specimens were 400mm in height and consisted of 35mm x 200mm Spruce-Pine-Fir (SPF) No.1/2 flanges connected to 40mm x 160mm Douglas Fir-Larch (D.Fir-L.) webs using a screw-glued connection. The connection consisted of 6mm diameter (dia.) x 100mm long partially threaded self-tapping screws (STS) with washer heads spaced at 133mm centre-to-centre (c/c), as well as a 10mm wide bead of commercially available silane modified construction adhesive (Figure 2). A 10mm wide bead of adhesive to every 40mm wide of web surface area was deemed adequate to provide full-surface coverage and adequate squeeze out.



*Figure 2: Dimensional Lumber Shear Test Specimens*

Additionally, 25mm dia. washers were added beneath the existing washer heads of the screws as a measure to aid in evenly spreading the pressure distribution of the screw-gluing as well as to prevent local wood crushing under the

screw heads (Figure 2). This assembly of partially threaded screw and 25mm dia, washer was able to achieve a load of 4.5kN [13], resulting in an average clamping stress of 0.85MPa. The flanges were sourced from a local Ontario wood supplier whereas the webs were removed from an existing building in Waterloo, Ontario Canada and donated to the University. In their original size, the web members had widths varying from 88 to 90mm to depths of 195-200mm. To maximize the use of wood, each element was planed to the final web dimensions thus yielding two webs per piece of wood donated. It should also be noted that the adhesive used complies with existing regulatory strength and durability requirements as a sub-floor adhesive [14].

A 500kN universal testing machine was used to evaluate the screw-glued bond performance of the four specimens under monotonic loading. The slip between the web and flange was recorded using a linear variable displacement transducer (LVDT) on both sides of the web and the average slip between the LVDTs was used in the stiffness calculation.

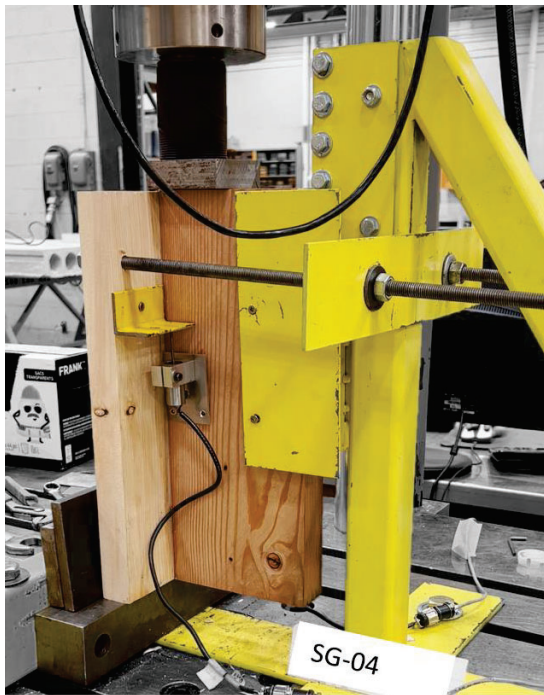


Figure 3: Shear connection test setup

The Standard Test Method for Strength Properties of Adhesive Bonds in Shear by Compression Loading (ASTM D905) [15] specifies a uniform loading rate of 5mm/min  $\pm$  25%, although the standard also states that there is no apparent effect on the bond strength for loading rates ranging 0.38 to 10.27mm/min. Additionally, the standard Test Methods for Mechanical Fasteners in Wood and Wood-Based Materials (ASTM D1761) [16] proposes a loading rate of 2.54 mm/min  $\pm$  25%. Due to the shear connection being comprised of adhesive and screws, a loading rate of 2mm/min was chosen which resulted in times to failures on average of 1.5 to 2 minutes. As shown

in Figure 3, the flange of the test specimen rested on a solid steel block that was secured to the testing frame, while a reaction frame (yellow), with a roller along the web, was used to resolve the eccentricity between the load application point and flange bearing location. Two steel bolts with a steel plate were also used to prevent rotation if any local crushing occurred beneath the flange.

Following each test, the moisture of both the flanges and web were determined using a Tramex MRH3 pin-probe moisture and relative humidity meter. The webs and flanges had an average moisture content of 9.2% and 11.2% respectively, with a maximum deviation of  $\pm$ 1% moisture. To determine the specific gravity, smaller clear wood elements were cut off the flange and web of each of the shear specimens. The clear wood specimens were then oven-dried according to Density and Specific Gravity (Relative Density) of Wood and Wood-Based Materials (ASTM D4442) [17] in order to determine the specific gravity of each. The D.Fir-L web elements had an average specific gravity of 0.47 with a coefficient of variation (CoV) of 0.02, while the SPF flange elements had an average specific gravity of 0.40 with CoV of 0.05.

## 2.2 EXPERIMENTAL TEST RESULTS

From the experimental tests, three key parameters were determined for each specimen: 1. the maximum load averaged over to glue area to determine the glue bond shear strength, 2. the slip stiffness ( $k_s$ ), and 3. the stiffness up until the maximum load ( $k_{Fmax}$ ). Table 1 presents the individual and average values of the screw-glued connections as well as their CoV.

Table 1. Shear connection load-slip results

Specimen	Shear Strength [MPa]	Slip Stiffness, $k_s$ [N/mm per mm <sup>2</sup> ]	Connection Stiffness at Max Load, $k_{Fmax}$ [N/mm per mm <sup>2</sup> ]
SG-01	4.69	19.11	18.78
SG-02	5.85	15.55	13.29
SG-03	3.89	15.94	12.11
SG-04	3.43	19.91	16.29
<b>Avg.</b>	<b>4.47</b>	<b>17.63</b>	<b>15.12</b>
CoV	0.20	0.11	0.17

The slip stiffness (i.e., initial stiffness), which is key when designing MTCs for service level and vibration criteria, was determined as the slope between 10% and 40% of the maximum load as defined by EN 26891 [18,19] for mechanical fastener connections. The connection stiffness at maximum load ( $k_{Fmax}$ ) was determined as the slope from the origin to the maximum load.

The shear strength of the screw glued bond averaged 4.47MPa, with a CoV 0.20. The high glue bond shear strength is a promising result as it indicates the composite connection can likely be designed for the strength of the wood material. The variation seen in the CoV of the shear



strength was attributed to specimens SG-02 and SG-04 where the difference in failure mode between these two specimens in the post glue bond failure observation can be seen presented in Figure 4. SG-02 (Figure 4a) shows a failure of wood fibre from both the web and flange indicating that the flange had a similar strength to the web, whereas for SG-04, the failure occurred almost entirely in the flange. Additionally, some wood decay was observed in the web at the top of the connection, as highlighted in Figure 4b.



(a) Failure plane of SG-02



(b) Failure plane of SG-04

**Figure 4:** Representative failure of screw-glued shear connection

In general, it is observed from Table 1 that the slip stiffness had less variation than the maximum load and provides encouraging results for the overall repeatability

of the screw-glued connection given the number of variables that can influence the overall behaviour (e.g., lumber grade, stiffness, surface planning, glue vs. wood failure, moisture content, curing conditions).

Determining the yield point of timber-timber composites is another key parameter needed for design calculations. Two bilinear load deformations models were data fitted to each specimen and the bilinear models were then averaged together to obtain a representative bilinear model for the screw-glued connection. The first bilinear model used the methodology presented in EN 12512 [20], and although intended for joints made of mechanical fasteners, this method provided good representation for the behaviour of the screw-glued connection. In the EN 12512 model [20], two sloped lines are determined, with their intersection being the yield point. The first line is defined by the slip stiffness from Table 1, while the second line is a tangent with a slope based on Equation (1).

$$\tan \beta = \frac{1}{6} \tan \alpha \quad (1)$$

Where  $\alpha$  is the angle formed by the slip stiffness line, and  $\beta$  is the angle formed by the tangent line. The tangent line is drawn on the load-slip curve where the slope of the tangent and load-slip curve are equal. The second bilinear model was proposed for its simplicity and relatively good agreement with the test data. Here, the yield point is determined where the slip stiffness line attains 75% of the maximum load. The second slope is then drawn between the yield point and maximum load point. Both models are demonstrated for specimen SG-04 in Figure 5: Load-slip curve of SG-04 with bilinear models.

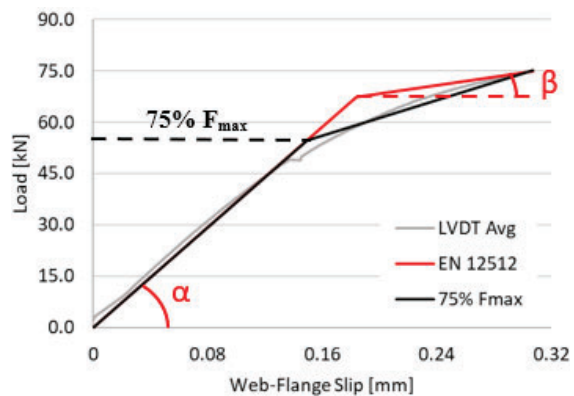


**Figure 5:** Load-slip curve of SG-04 with bilinear models

The average curves for the four specimens are presented in Figure 6, with the yield point results in Table 2. Generally, both models capture the behaviour well, with the EN 12512 [20] having a higher yield stress.

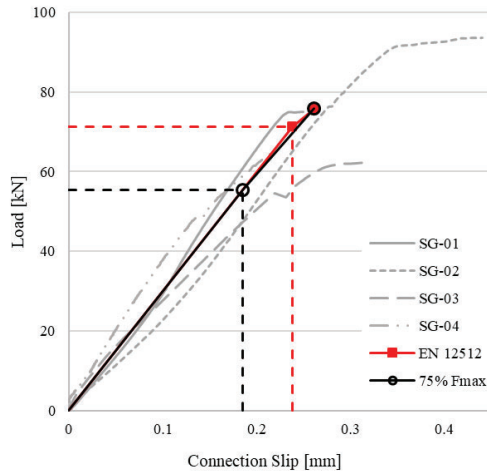


**Figure 6:** Load-slip curves and averaged bilinear models

The yield stress was determined by dividing the data fit yield load for each specimen by the 40mm x 400mm screw-glued area. Some variation is seen in the slip and load of the yielding point. This can be attributed to the variability in wood material shear strength, as well as stiffness, and its influence of the glue bond behaviour. The average yield stresses of 4.59 MPa and 3.47 MPa demonstrate the potential for structural viability of a screw-glued connection using a commercially available bead extruded silane modified adhesive by primarily achieving failure in the wooden elements first, as opposed to a pure glue failure being the dominating failure mode.

**Table 2.** Yield point using bilinear models

Specimen	EN 12512		75% F <sub>max</sub>	
	Yield Slip [mm]	Yield Stress [kN]	Yield Slip [mm]	Yield Stress [kN]
SG-01	0.222	4.67	0.167	3.52
SG-02	0.336	5.76	0.256	4.39
SG-03	0.234	3.73	0.183	2.92
SG-04	0.184	4.20	0.132	3.04
<b>Avg.</b>	<b>0.244</b>	<b>4.59</b>	<b>0.185</b>	<b>3.47</b>
<b>CoV</b>	<b>0.26</b>	<b>0.18</b>	<b>0.24</b>	<b>0.17</b>

### 3 DIMENSIONAL LUMBER T-BEAM BENDING TESTING

#### 3.1 METHODOLOGY

The dimensional lumber T-beams were 2m in length with a 1.8m clear span and consisted of an identical 35mm x 200mm SPF No.1/2 flange as well as a 40mm x 160mm D.Fir-L. web compositely connected using the screw-glue configuration tested in Section 2. Prior to each of the T-beams being assembled, the web and flange elements were each tested non-destructively to determine the modulus of elasticity, E. This was done by loading the elements in their T-beam orientation (i.e., the flanges on the flat and the webs on edge) in four-point bending and

recording the midspan deflection using a string pot. The actuator load was increased up to 10kN and 2kN for the webs and flanges, respectively, to obtain a representative linear load-displacement curve to calculate the modulus of elasticity for each using classical Euler beam theory. However, since the midspan deflections recorded included deformations due to shear which results in the apparent modulus of elasticity, E<sub>app</sub>. To get the true modulus of elasticity (i.e., shear free), E<sub>true</sub>, additional analysis was required. Equation (2) was used to remove the shear deformations from the midspan deflection, where E<sub>true</sub> could then be calculated using classical Euler beam theory.

$$\Delta_{shear} = \frac{P}{3AG}L \quad (2)$$

Where P is the actuator load, L is the clear span of the specimen (1.8m), A is the cross-sectional area, and G is the shear modulus taken as E<sub>app</sub>/15 for the webs and E<sub>app</sub>/18 for the flanges based on the lumber species and recommendations from Forest Products Laboratory's Wood handbook [21]. The results from the modulus of elasticity determination are presented in Section 3.2 in Table 3.

A total of six-dimensional lumber T-beams were assembled and loaded in four-point bending using the test setup shown in Figure 7. During the testing, the displacement at midspan was monitored using a string pot which passed through the table, while the slip between the web and flange was recorded using LVDTs located 0.3m and 0.6m from the midspan of the beams. Similar to the modulus of elasticity determination, the midspan deflection was used to determine the apparent and true stiffness of the beams, EI<sub>app</sub> and EI<sub>true</sub> respectively, based on the linear portion of the load-displacement curve.

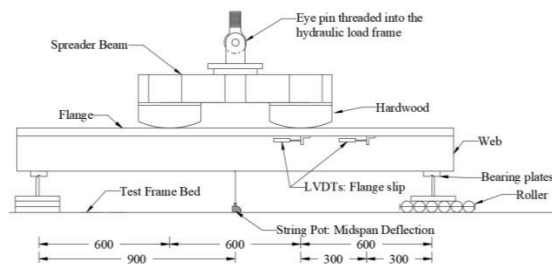


**Figure 7:** Four-point bending test setup

#### 3.2 EXPERIMENTAL TEST RESULTS

The results from the modulus of elasticity determination for the flange and web elements of each beam are presented in Table 3. Overall, the flanges' modulus of elasticity was very consistent was an average E<sub>true</sub> of 9062MPa, while more variability was seen in the average E<sub>true</sub> of the webs of 13430MPa. This higher variation is attributed to the fact that the final web size was obtained by planing the original member to their final size, thus affecting the distribution of defects and grain deviation from member to member.

**Table 3:** Modulus of elasticity results

Specimen	Flange*		Web	
	E <sub>app</sub> [MPa]	E <sub>true</sub> [MPa]	E <sub>app</sub> [MPa]	E <sub>true</sub> [MPa]
SG-01	9219	9268	8485	9350
SG-02	8408	8452	10473	11375
SG-03	9781	9833	11172	12197
SG-04	9748	9800	15600	17409
SG-05	8102	8146	12822	14128
SG-06	8828	8875	14630	16121
<b>Avg.</b>	<b>9014</b>	<b>9062</b>	<b>12197</b>	<b>13430</b>
CoV	0.07	0.07	0.21	0.20

\*Flange modulus of elasticity measured on flat

Key results describing the properties of each of the T-beams section are presented in Table 4. The maximum bending moment was determined by the maximum load reached in the test after the initial linear-elastic region of the load-displacement response. The average of this was 10.8kNm. However, considerable variation was observed and can primarily attributed to the variable grade of wood in the webs. Due to planing of the donated material into the final web sizes, some of them had less grain deviation and fewer defects as well as knots than others, thus resulting in increased flexure and shear strength in these specimens.

**Table 4:** T-beam bending experimental results

Specimen	Max Bending Load	Apparent Stiffness, EI <sub>app</sub>	True Stiffness, EI <sub>app</sub>
	[kNm]	[Nmm <sup>2</sup> ]	[Nmm <sup>2</sup> ]
SG-01	6.4	3.12E+11	3.96E+11
SG-02	13.7	3.33E+11	4.08E+11
SG-03	9.7	3.12E+11	3.72E+11
SG-04	10.3	4.21E+11	4.99E+11
SG-05	15.3	4.32E+11	5.03E+11
SG-06	9.4	4.07E+11	4.64E+11
<b>Avg.</b>	<b>10.8</b>	<b>3.69E+11</b>	<b>4.40E+11</b>
CoV	0.27	0.14	0.12

Nonetheless, lower CoVs were observed for the apparent and true stiffness of the sections. These are the primary focus of the experimental program as it is used in the comparison to the numerical modelling in Section 4, while also being indicative of the serviceability-level response, a key concern for future application in mass timber composites. The average apparent and true stiffness of the sections were found to be  $3.69 \times 10^{11} \text{Nmm}^2$  and  $4.40 \times 10^{11} \text{Nmm}^2$  respectively. Most of the variability in these results was attributed to the different modulus of elasticity of the webs, as the web modulus of elasticity was generally indicative of the overall stiffness of the assembly (i.e., T-beam). For example, lower modulus of elasticity sections such as SG-01 and SG-02 had lower overall assembly stiffnesses than the ones with higher modulus of elasticity sections such as SG-04 and SG-05. The experimental load-displacement curves of all six specimens are presented in Figure 8.

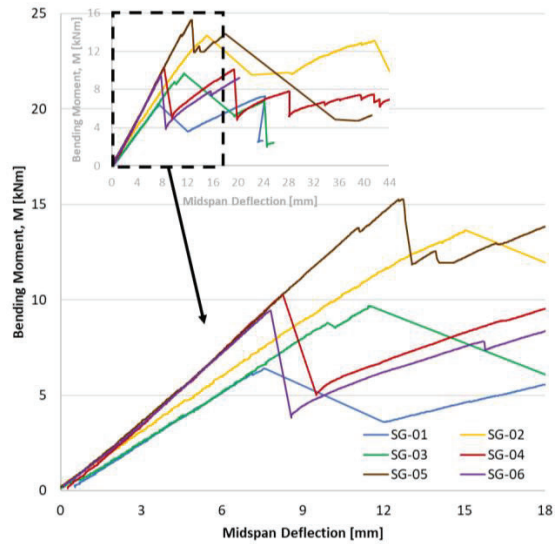


**Figure 8:** T-beam load-displacement curves

In general, due to the relatively short spans and increase section modulus of the T-section, the initial failure mode consisted of shear failure in the webs. This was followed by secondary flexural failures such as simple, splintering, and cross-grain tension in the web, while failure of the flanges was observed to either be due to compression yielding or simple tension. Figure 9 shows a representative T-beam at ultimate failure.



**Figure 9:** Representative failure mode of T-beams

## 4 NUMERICAL ANALYSIS

### 4.1 NUMERICAL MODEL DESCRIPTION

A numerical model was developed in *ABAQUS* finite element software [22] to capture the behaviour of the dimensional lumber T-beams and screw-glued connection. The assembly was generated using three separately defined elements; the SPF flange, the D.Fir-L web, and the loading blocks shown in Figure 10. The flange and web were modelled as 3D deformable solids, while the loading blocks were modelled as 3D rigid elements. The contact between the webs and flanges was modelled as a cohesive contact in the sliding direction and a “hard” contact in the normal direction. Boundary conditions were applied at the support locations

restricting all degrees of freedom except in-plane rotation, and in-plane displacement representing the roller end. The slip stiffness of the screw-glued bond,  $k_s$ , was used as the in-plane slip of the cohesive bond in the numerical model. Contact between the T-beam and the support blocks was modelled as a “hard” contact in the normal direction and a frictional penalty coefficient of 0.15 [23] in the tangential direction.

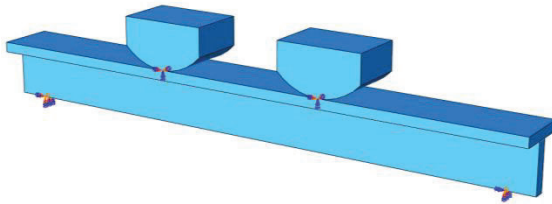


**Figure 10:** Finite element model showing T-beam below two loading blocks and boundary conditions applied

The wood elements are modelled as a linear-elastic orthotropic material using ABAQUS’ engineering constants option, where the primary direction (1) represents the longitudinal direction of the wood grain and the two secondary directions (2) and (3) represent the two perpendicular to grain directions (i.e., radial and tangential). The experimentally determined true modulus of elasticity for each web and flange is used for the longitudinal modulus of elasticity,  $E_1$ , while the shear modulus  $G_{12}$  and  $G_{13}$  is taken as  $E_{true}/15$  for the webs and  $E_{true}/18$  for the flanges based on the lumber species and recommendations from Forest Products Laboratory’s Wood handbook [21]. The Poisson ratios were also based on recommendations for each species group from Forest Products Laboratory’s Wood handbook [21]. The remaining  $E_2$ ,  $E_3$ , and  $G_{23}$  are based on CSA O86 [24] recommended values in term of  $E_{true}$ . The material parameters are summarized in Table 5.

**Table 5:** Material parameter values used in ABAQUS model

	Web Element	Flange Element
$E_1$ (MPa)	$E_{true,web}$	$E_{true,flange}$
$E_2$ (MPa) <sup>1</sup>	$E_1/30$	$E_1/30$
$E_3$ (MPa) <sup>1</sup>	$E_1/30$	$E_1/30$
$\nu_{12}$	0.32	0.35
$\nu_{13}$	0.35	0.35
$\nu_{23}$	0.39	0.45
$G_{12}$ <sup>2</sup> (MPa)	$E_1/15$	$E_1/18$
$G_{13}$ <sup>2</sup> (MPa)	$E_1/15$	$E_1/18$
$G_{23}$ <sup>3</sup> (MPa)	$G_{12}/10$	$G_{12}/10$

## 4.2 COMPARISON OF EXPERIMENTAL AND NUMERICAL RESULTS

The numerical model was run for each T-beam specimen, with the corresponding combination of web and flange true modulus of elasticity, in order to validate the

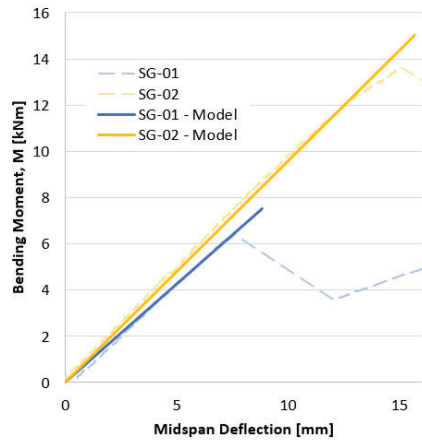
numerical results against the experimental results. For each T-beam, a specific bending moment and displacement point corresponding to an initial failure and the transition from linear-elastic to non-linear were carefully selected for comparison to the model. Thus, the loading in the model was increased until it reached the specific bending moment,  $M_{specified}$ , and then the experimental and numerical displacements were compared. The results of this comparison are summarized in Table 6. It should be noted the numerical model was limited to the linear-elastic stiffness of the T-beams and did not aim to predict ultimate failure.

**Table 6:** Comparison of experimental (Exp.) and FE model deflections at midspan based on specified bending moment

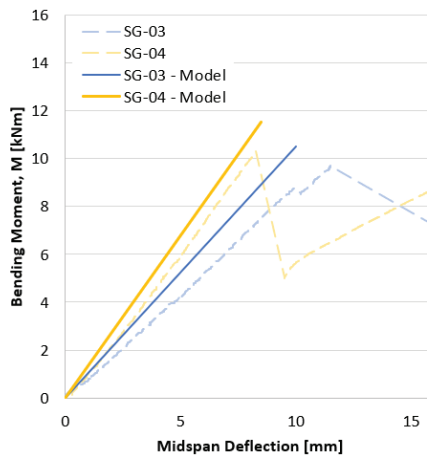
Specimen	$M_{specified}$ [kNm]	Exp. Deflection [mm]	FE Model Deflection [mm]	Exp./FE Model [-]
SG-01	6.0	6.98	7.06	1.01
SG-02	10.8	11.15	11.27	1.01
SG-03	7.8	8.78	7.42	0.85
SG-04	9.9	7.95	7.30	0.92
SG-05	12.9	10.35	11.58	1.12
SG-06	9.0	7.42	7.18	0.97
			<b>Avg.</b>	<b>0.98</b>
			CoV	0.09

The numerical model agreed reasonably well with the experimental model, with the average experimental midspan deflection being 0.98 of the numerical midspan deflection with a CoV of 0.09. The deviation in SG-03 and SG-05 is not uncommon for dimensional lumber and can partially be attributed to the presence of localized defects in the wooden elements, lack of a continuous bond, and appreciable error in the properties (e.g., average slip stiffness used). The load-displacement curve for each of the experiment specimens, along with the numerical model response is presented in Figure 11: Load-deformation curve from experimental and numerical model results. Overall, the numerical model was deemed capable of capturing the screw-glued shear connection behaviour.

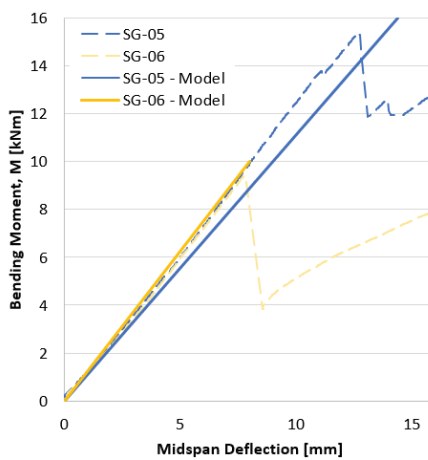




(a) T-beam SG-01 and SG-02



(b) T-beam SG-03 and SG-04



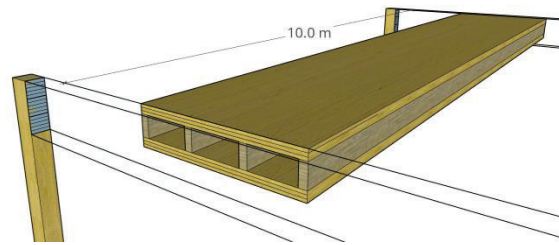
(c) T-beam SG-05 and SG-06

**Figure 11:** Load-deformation curve from experimental and numerical model results

## 5 IMPLICATIONS ON MASS TIMBER COMPOSITES

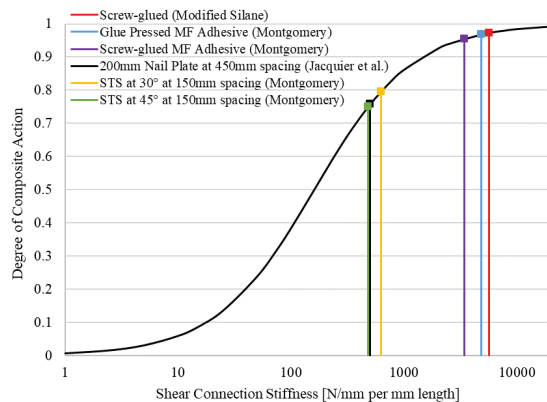
To investigate the feasibility of the shear-glued connection studied in the current paper for use in MTC panels, the experimentally determined slip stiffness from

Table 1 was analytically applied to a 10m long CLT-glulam HMT panel shown in Figure 12. The HMT panel consisted of four 80 x 245mm SPF 20f-E grade glulam webs and two 105 x 2400mm V2 grade CLT panels, with material properties taken from CSA O86 [24]. The  $\gamma$ -method, which has been shown to be an accurate method for determining the behaviour of MTCs in design [10,11], was used for this analysis.



**Figure 12:** 10m hollowcore mass timber panel

The results of the analysis are presented in Figure 13 where the screw-glued connection slip stiffness was able to achieve a high degree of composite action (>95%), thus resulting in an HMT panel that was able to meet the design criteria of a 10m span for stiffness requirements due to vibration demands. For comparison, a few select connections experimentally tested on CLT-glulam shear specimens by Montgomery [6] and Jacquier [10] are also presented in Figure 13.



**Figure 13:** Degree of composite action in HMT panel based on shear connection stiffness

For the screw-glued connection, the HMT panel achieved a stiffness of approximately  $105 \times 10^{12} \text{ Nmm}^2$  which corresponded to a vibration-controlled span, according to the CSA O86 Annex A clause A8.5.3 [24] for the vibration-controlled span of CLT panels, of 10.4m. Overall, this indicated that the commercially available bead extruded silane modified adhesive and partially threaded STS is an easily applied, and structurally viable screw-glued connection for MTC panels, able to achieve high degrees of composite action.



## 6 CONCLUSIONS AND FUTURE WORK

Presented herein are the results of an experimental study investigating the behaviour of a screw-glued connection, with the goal of justifying it as a structurally viable shear connection for MTC panels. The connection consisted of 6mm dia. x 100mm long partially threaded STS with washer heads spaced at 133mm c/c, as well as a 10mm wide bead of commercially available silane modified construction adhesive on a 40mm wide web. Additionally, 25mm dia. washers were added beneath the existing washer heads of the screws as a measure to aid in evenly spreading the pressure distribution of the screw-gluing, as well as to prevent local wood crushing under the screw heads. The results have shown that the screw-glued connection was able to achieve a slip modulus of 17.63 N/mm per mm<sup>2</sup> of glue with a CoV of 0.11. The lower level of variation in the connection stiffness is encouraging for the overall repeatability of the screw-glued connection given the number of variables that can influence the overall behaviour (e.g., lumber grade, stiffness, surface planning, glue vs. wood failure, moisture content, curing conditions). Overall, when used on a 10m HMT panel, analytical results using the  $\gamma$ -method indicated a nearly fully composite shear connection was achieved and a vibration-controlled span of 10.4m was possible for the 455mm deep section.

Two bilinear models were used to represent the load-slip response and to determine the yield stress of the screw-glued connection. The first, based on EN 12512, provided an average yield stress of 4.59MPa while the second, based on yield occurring at 75% of the maximum load, provided an average yield stress of 3.47MPa.

The average apparent and true stiffness of the sections were found to be  $3.69 \times 10^{11}$  Nmm<sup>2</sup> and  $4.40 \times 10^{11}$  Nmm<sup>2</sup> respectively, with most of the variation in stiffness across specimens attributed to the different modulus of elasticity of the webs. Generally, higher webs stiffnesses were proportional to higher T-beam section stiffnesses. The experimental T-beam results were then compared to a FE model created to capture the behaviour. For each T-beam flange and web element, the modulus of elasticity was determined not destructively and used as input for the model. Overall, the numerical model agreed well with the numerical model, with the average experimental midspan deflection being 0.98 of the numerical midspan deflection with a CoV of 0.09. The numerical model was thus deemed likely capable of capturing the screw-glued connection behaviour and will be used on future numerical analysis of MTCs.

The screw-glued connection investigate herein has proven to be a structurally viable and easy to apply shear connection with great potential for use in MTC panels. Future work applies the current screw-glued connection, along with other promising shear connection candidates, to CLT-glulam shear specimens with the goal of determining the optimal connection based on connection stiffness and yield stress, constructability, and cost for use in the production of MTC panels in industry. The optimal

three connection configurations are used in the fabrication of 15 CLT-glulam T-beams which, to the author's knowledge, will be one of the largest studies on MTC panels.

## REFERENCES

- [1] Kirsten Lewis Rijun Shrestha, Keith Crews BB. The Use of Cross Laminated Timber for Long Span Flooring in Commercial Buildings. WCTE 2016 - World Conf. Timber Eng., 2016.
- [2] FPIInnovations. Canadian CLT Handbook. 2nd Editio. Pointe-Claire, Quebec: 2019.
- [3] WoodWorks - Wood Product Council. Case Study: Catalyst. Spokane, Washington, USA: 2020.
- [4] Element5 Co. WoodIn 2023. <https://elementfive.co/projects/woodin/>.
- [5] Hull T, Lacroix D. Analytical Investigation of the Potential of Hollowcore Mass Timber Panels for Long Span Floor Systems. In: Walbridge S, Nik-Bakht M, Ng KTW, Shome M, Alam MS, El Damatty A, et al., editors. Can. Soc. Civ. Eng. Annu. Conf. 2021, Singapore: Springer Nature Singapore; 2022, p. 621–33.
- [6] Montgomery WG. Hollow Massive Timber Panels: A High-Performance, Long-span Alternative to Cross Laminated Timber. Clemson University, 2014.
- [7] Chen Y, Lam F. Bending Performance of Box-Based Cross-Laminated Timber Systems. J Struct Eng 2013;139.
- [8] Jacquier N, Girhammar UA. Evaluation of bending tests on composite glulam-CLT beams connected with double-sided punched metal plates and inclined screws. Constr Build Mater 2015. <https://doi.org/10.1016/j.conbuildmat.2015.07.137>.
- [9] European Committee for Standardization (CEN). EN 1995-1-1:2004/A2:2014 – Eurocode 5 – Design of timber structures – Part 1-1: General – Common Rules and Rules for Buildings. Brussels, Belgium: European Committee for Standardization; 2014.
- [10] Jacquier N, Girhammar UA. Evaluation of bending tests on composite glulam-CLT beams connected with double-sided punched metal plates and inclined screws. Constr Build Mater 2015;95:762–73. <https://doi.org/10.1016/J.CONBUILDMAT.2015.07.137>.
- [11] Hull T, Lacroix D. Comparative analysis of the feasibility of hollowcore mass timber panels for long span floor systems. World Conf. Timber Eng., Santiago, Chile: 2021, p. 8.
- [12] Katarina Bratulic MA. Screw Gluing - Experimental and Theoretical Study on Screw Pressure Distribution and Glue Line Strength. WCTE 2016, 2016.
- [13] Rothoblass. Plates and Connectors for Timber Buildings. 2019.
- [14] ASTM. Standard Specification for Adhesives for

- Field-Gluing Wood Structural Panels ( Plywood or Oriented Strand Board ) to Wood Based Floor (D3498-19a). vol. i. 2019. <https://doi.org/10.1520/D3498-19a.2>.
- [15] ASTM. Standard Test Method for Strength Properties of Adhesive Bonds in Shear by Compression Loading. ASTM D905-21 2021.
- [16] ASTM. Standard Test Methods for Mechanical Fasteners in Wood and Wood-Based Materials. D1761-20 2020.
- [17] ASTM. Standard Test Methods for Direct Moisture Content Measurement of Wood and Wood-Based Materials (ASTM D4442). West Conshohocken, PA: 2020.
- [18] CEN. Timber Structures - Joints Made with Mechanical Fasteners - General Principles for the Determination of Strength and Deformation Characteristics (EN 26891) 1991:6.
- [19] Muñoz W, Salenikovich A, Mohammad M, Quenneville P. Determination of Yield Point and Ductility of Timber Assemblies: in Search for a Harmonised Approach. World Conf Timber Eng 2008;Volume 1.
- [20] CEN. Timber Structures - Test Methods - Cyclic Testing of Joints Made with Mechanical Fasteners (EN 12512) 2001:18.
- [21] Forest Products Laboratory. Wood handbook - Wood as an engineering material. Madison, WI: Forest Products Laboratory, USDA Forest Service,; 2010.
- [22] Dassault Systemes Simula Corp. ABAQUS [Computer software] 2020.
- [23] Koubek R, Dedicova K. Friction of wood on steel. Linnaeus University, 2014.
- [24] Canadian Standards Association. Engineering Design in Wood. CSA-O86 2019.